

MRI Optimization of Interventional Oncology Techniques

Jason Chiang, MD, PhD
Assistant Professor

Division of Interventional Radiology
Department of Radiological Sciences

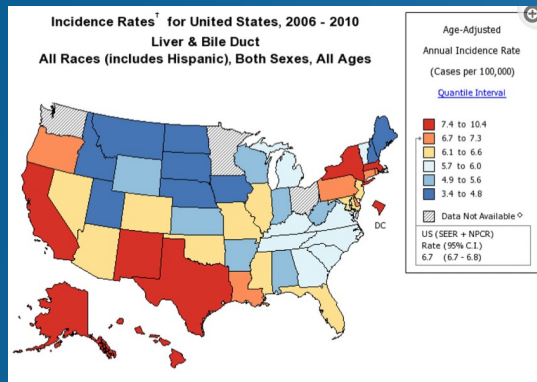
UCLA Ronald Reagan Medical Center, Los Angeles, CA

Disclosures



- J.C. receives licensing fees for patents relating to MWA through the Wisconsin Alumni Research Foundation; equipment support from Ethicon Neuwave Medical Inc.

Global Burden of HCC



- Hepatocellular carcinoma is one of the most common form of liver cancer with an estimated case incidence of >1 million by 2025
- Rates have tripled in the United States over the last 3 decades
- Hepatitis B and C are the main risk factors for HCC development, although NASH is becoming a bigger risk factor in the West.
- Asians and Hispanics have the highest incidence rates of HCC in the United States -> 1/3 live in CA. ~40/100,000 in CA alone

Llovet JM et al. Hepatocellular carcinoma. Nat Rev Dis Primers. 2021 Jan 21;7(1):6.

Han SS et al. . Changing Landscape of Liver Cancer in California: A Glimpse Into the Future of Liver Cancer in the United States. J Natl Cancer Inst. 2019 Jun 1;111(6):550-556.

Diagnosing HCC

Diagnosis, Staging, and Management of Hepatocellular Carcinoma: 2018 Practice Guidance by the American Association for the Study of Liver Diseases

Jorge A. Marrero,¹ Laura M. Kulik,² Claude B. Sirlin,³ Andrew X. Zhu,⁴ Richard S. Finn,⁵ Michael M. Abecassis,² Lewis R. Roberts,⁶ and Julie K. Heimbach⁶

Diagnosis

2. The AASLD recommends diagnostic evaluation for HCC with either multiphase CT or multiphase MRI because of similar diagnostic performance characteristics.

Quality/Certainty of Evidence: Low for CT versus MRI

Strength of Recommendation: Strong

LR-1	Definitely benign
LR-2	Probably benign
LR-3	Intermediate probability of malignancy
LR-M	Probably HCC
LR-4	
LR-5	Definitely HCC

CT/MRI Diagnostic Table

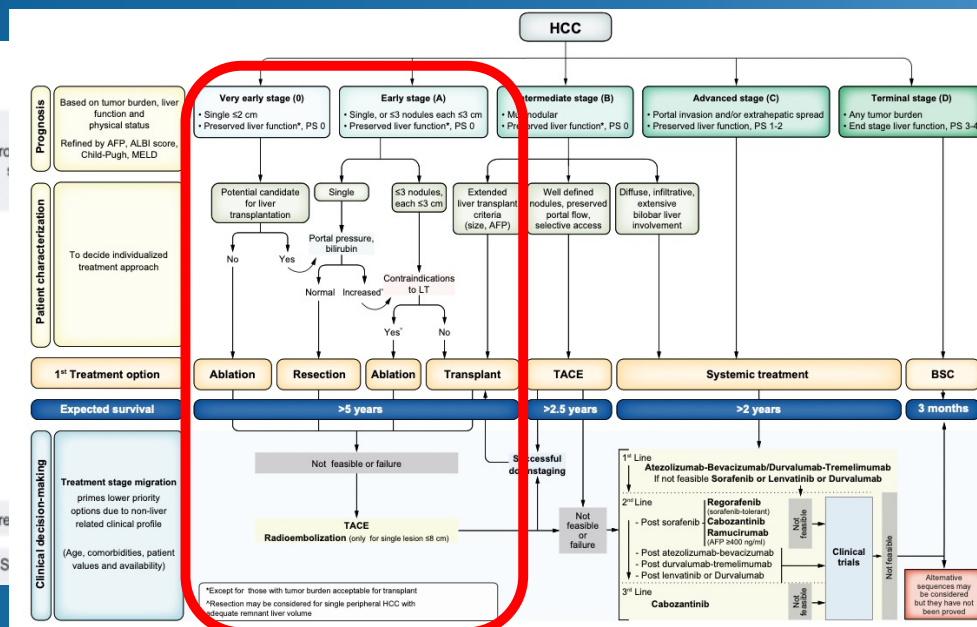
Arterial phase hyperenhancement (APHE)		No APHE		Nonrim APHE		
Observation size (mm)		< 20	≥ 20	< 10	10-19	≥ 20
Count additional major features: • Enhancing "capsule" • Nonperipheral "washout" • Threshold growth	None	LR-3	LR-3	LR-3	LR-3	LR-4
	One	LR-3	LR-4	LR-4	LR-4 / LR-5	LR-5
	≥ Two	LR-4	LR-4	LR-4	LR-5	LR-5



Observations in this cell are categorized based on one additional major feature:

- LR-4 – if enhancing "capsule"
- LR-5 – if nonperipheral "washout" **OR** threshold growth

BCLC guidelines

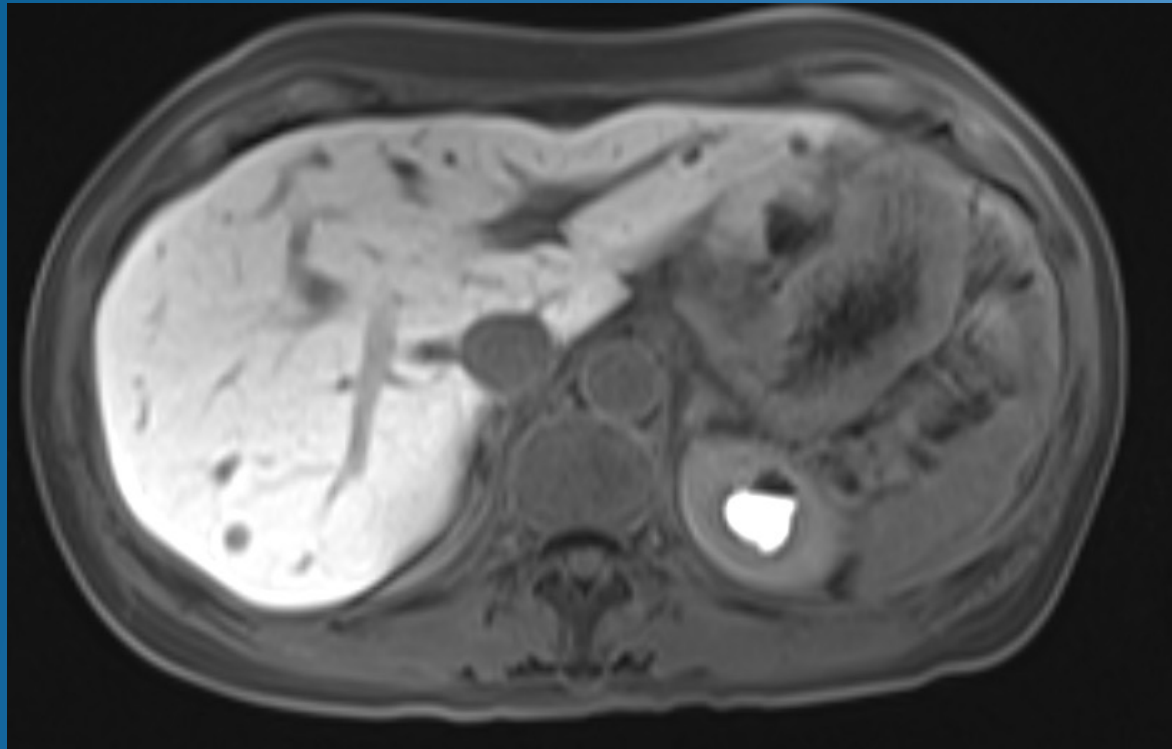


Reig M, Forner A, Rimola J, Ferrer-Fàbrega J, Burrel M, Garcia-Criado Á, Kelley RK, Galle PR, Mazzaferro V, Salem R, Sangro B, Singal AG, Vogel A, Fuster J, Ayuso C, Bruix J. BCLC strategy for prognosis prediction and treatment recommendation: The 2022 update. J Hepatol. 2022 Mar;76(3):681-693.

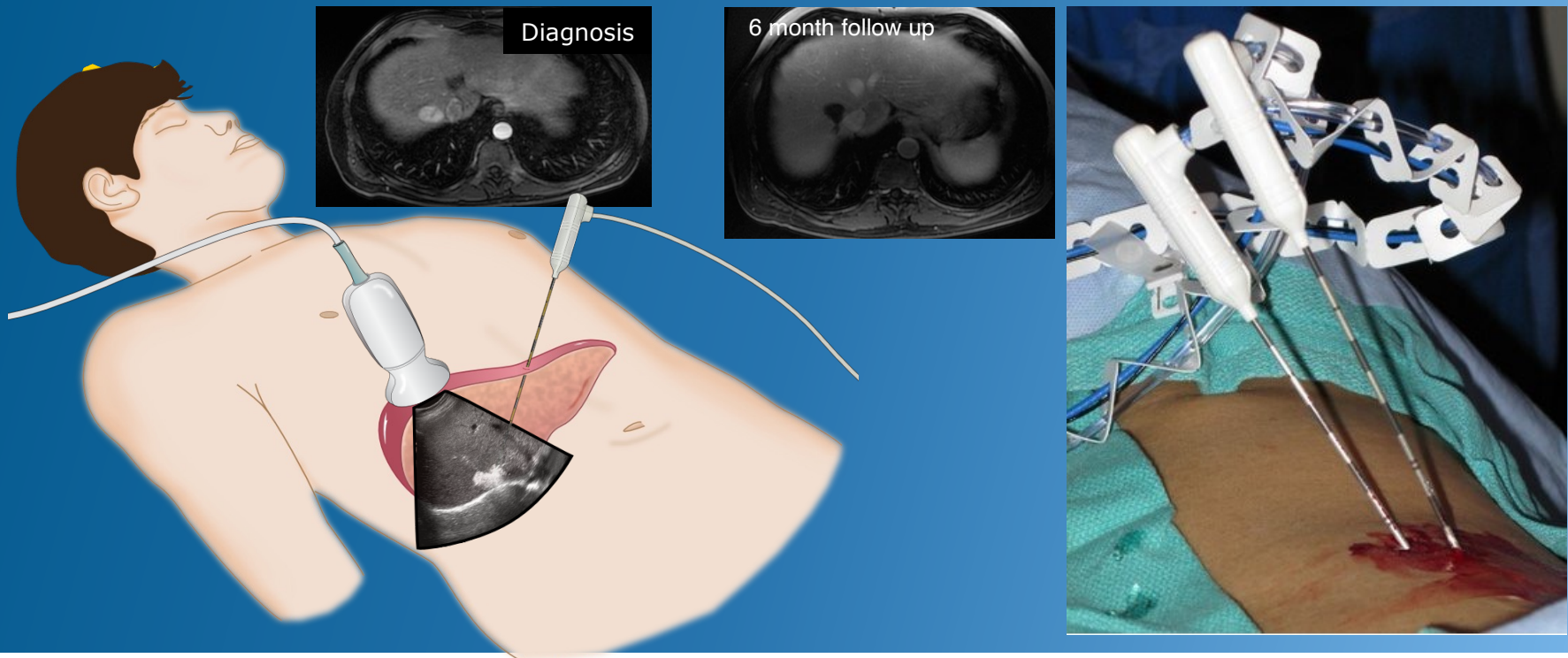
Cross Sectional Imaging: MRI Abdomen



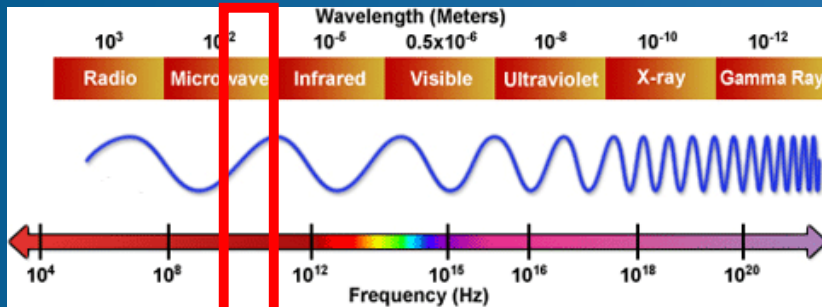
Case Example: Diagnostic evaluation



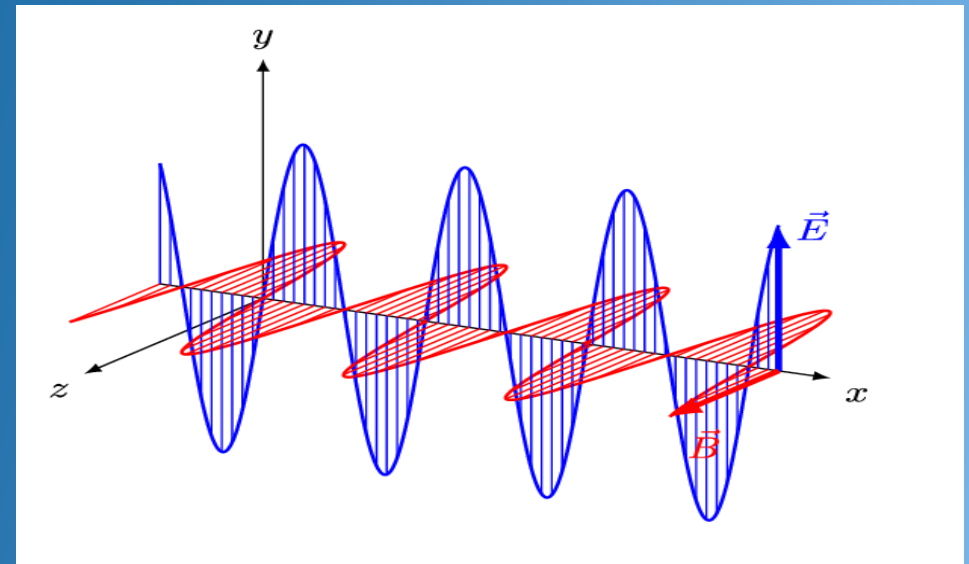
How do we do ablations?



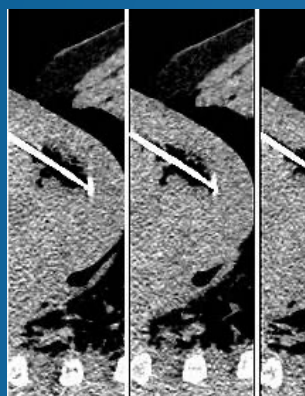
MWA vs RF: Differences in energy source



915 MHz
2.45 GHz



Ablation planning and treatment



Variables at play:

- Tissue type
- Physiology
- Operator mechanics
- MWA antenna design

tumor size

visualize anatomy

visualize trajectory.

Follow manufacturer guidelines

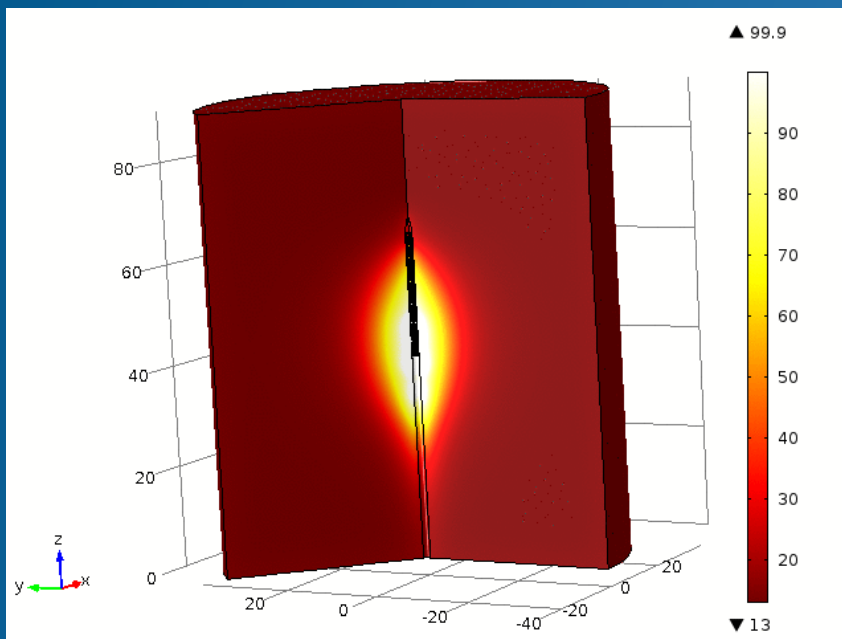


Insufficient Heating

Technically
successful
ablation

Excess heating

Benefits of computational modeling

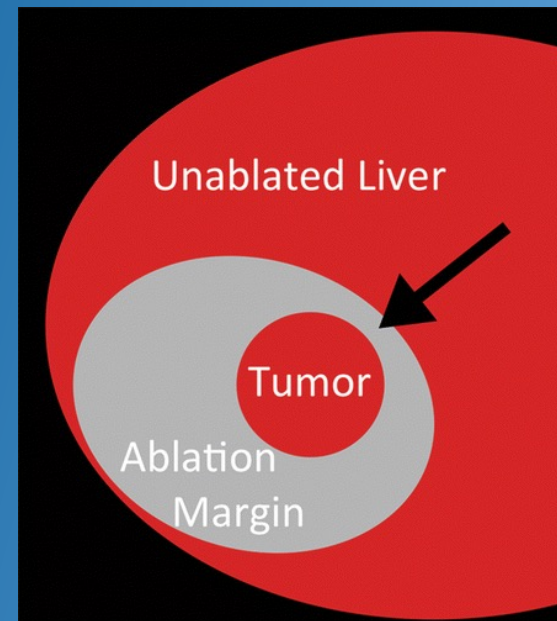
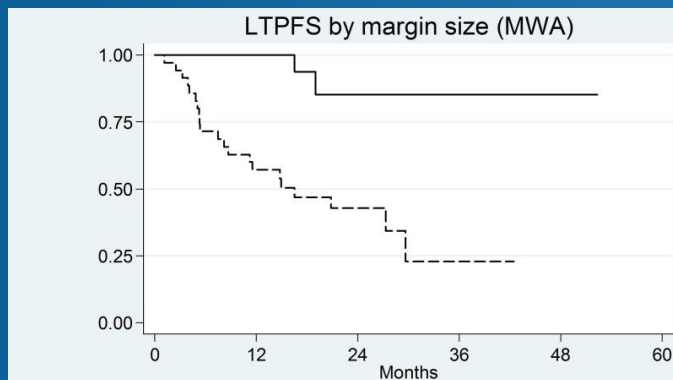


Create a highly controlled environment to investigate and understand the effects of changing individual input variables

- Laboratory Work
 - More **focused** experimental studies
 - **Fewer** animal studies
 - **Decreased** developmental costs
 - **Greater research** efficiency
- Clinical Work
 - Tailor treatment to **patient-specific** environments
 - Optimize device settings before a procedure

Margins are critical – use modeling to help you predict it ahead of time!

Margin	LTP rate
≤ 5 mm	60% (21/35)
5-10 mm	10.5% (2/19)
>10 mm	0% (0/6)



Shady, Waleed, Elena N. Petre, Kinh Gian Do, Mithat Gonen, Hooman Yarmohammadi, Karen T. Brown, Nancy E. Kemeny, et al. "Percutaneous Microwave versus Radiofrequency Ablation of Colorectal Liver Metastases: Ablation with Clear Margins (A0) Provides the Best Local Tumor Control." *Journal of Vascular and Interventional Radiology* 29, no. 2 (February 2018): 268-275.e1.

Modeling ablations: Basics in heat transfer

Ablation Modality	Max temperature	Mechanism of Heating	Risk:
Radiofrequency Ablation	<100 °C	Thermal Conduction	Insufficient heat, higher recurrence rate



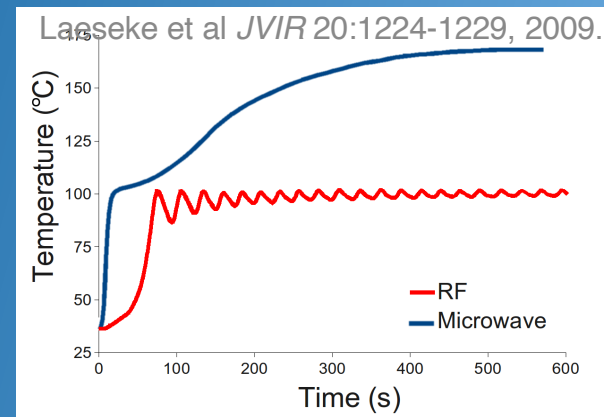
$$P_{\text{conduction}} = \frac{Q}{t} = kA \frac{T_h - T_c}{L}$$

Modeling MWA: Mechanism of heating

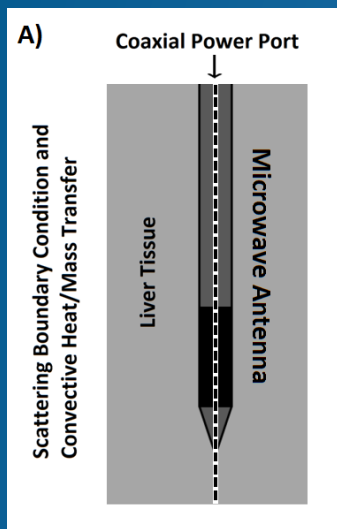
Ablation Modality	Max temperature	Mechanism of Heating	Risk:
Microwave Ablation	>100 °C	Thermal Conduction + Active Heating + Water Vapor	Inadvertent damage, thrombosis

Factors that make MWA amenable to modeling

- Tissue-specific heating based on antenna design
- Less susceptibility to the heat-sink effect



Basic computational setup and output

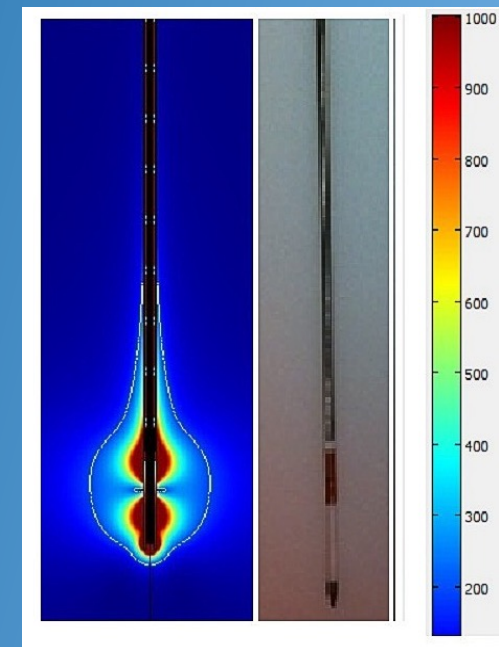


- 1) Solve Maxwell's equation to get time-dependent electromagnetic field propagation

$\nabla \cdot \mathbf{D} = \rho$	(1)	Gauss' Law
$\nabla \cdot \mathbf{B} = 0$	(2)	Gauss' Law for magnetism
$\nabla \times \mathbf{E} = -\frac{\partial \mathbf{B}}{\partial t}$	(3)	Faraday's Law
$\nabla \times \mathbf{H} = \frac{\partial \mathbf{D}}{\partial t} + \mathbf{J}$	(4)	Ampère-Maxwell Law

- 2) Solve for heat generation from electric field vector

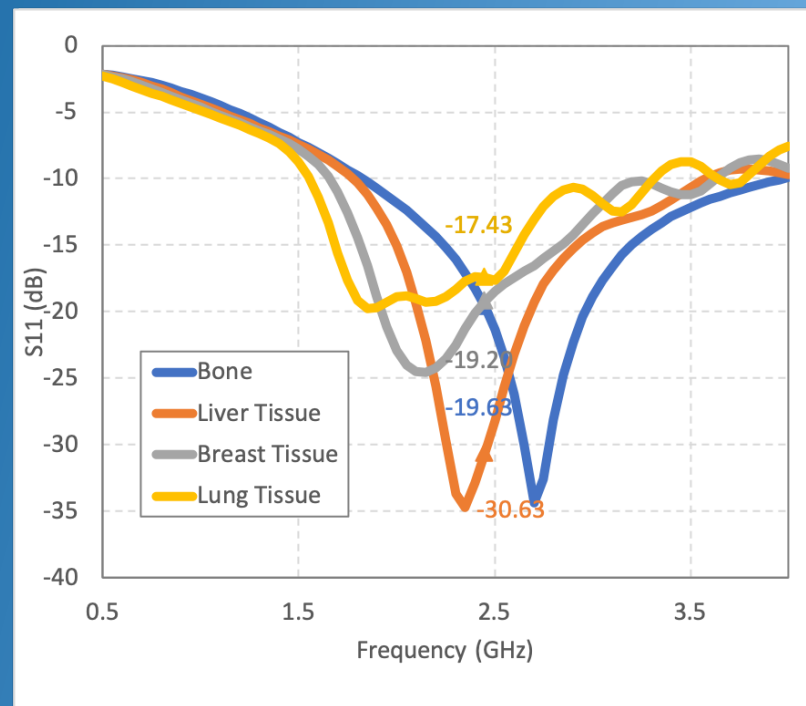
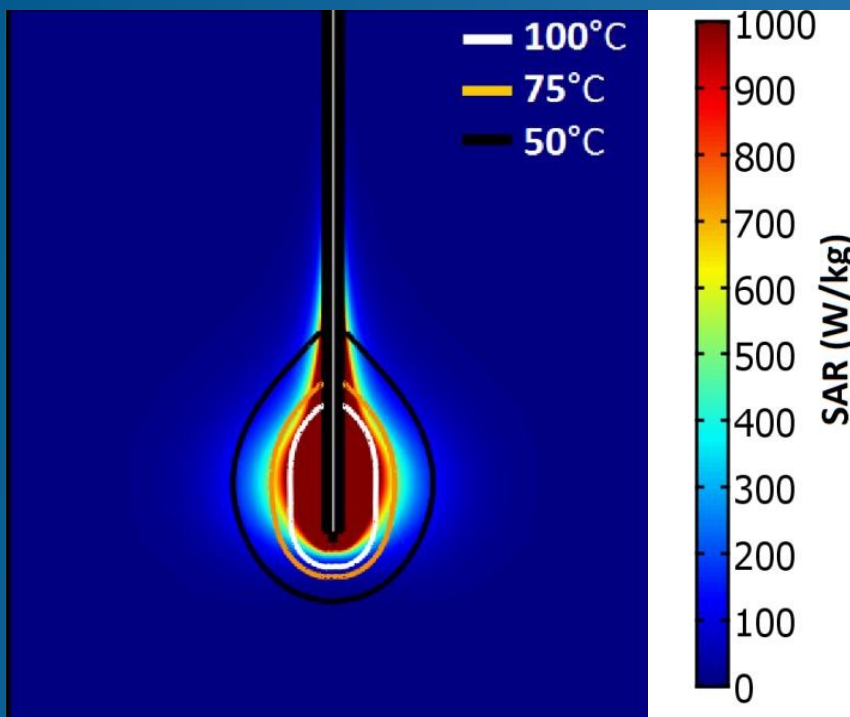
$$Q = \frac{1}{2} \sigma |\mathbf{E}|^2 \quad (\text{W/m}^3)$$



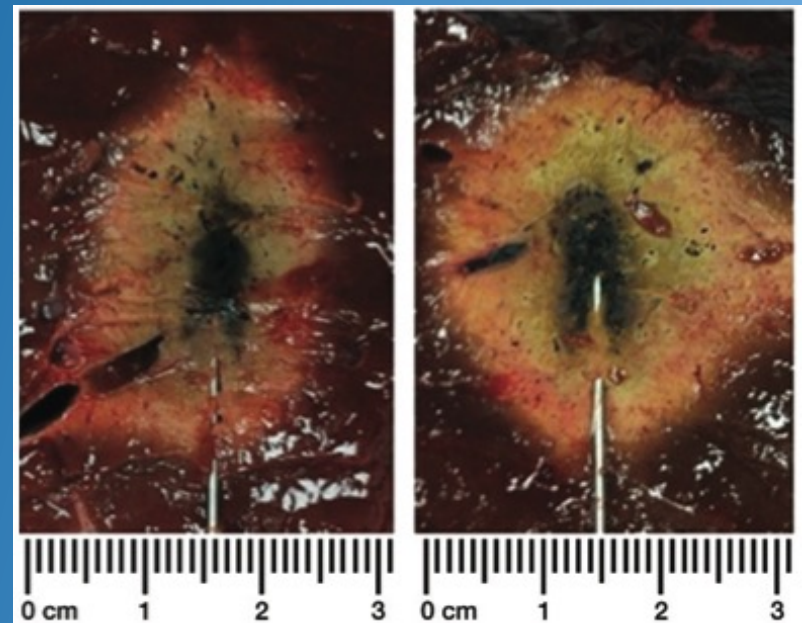
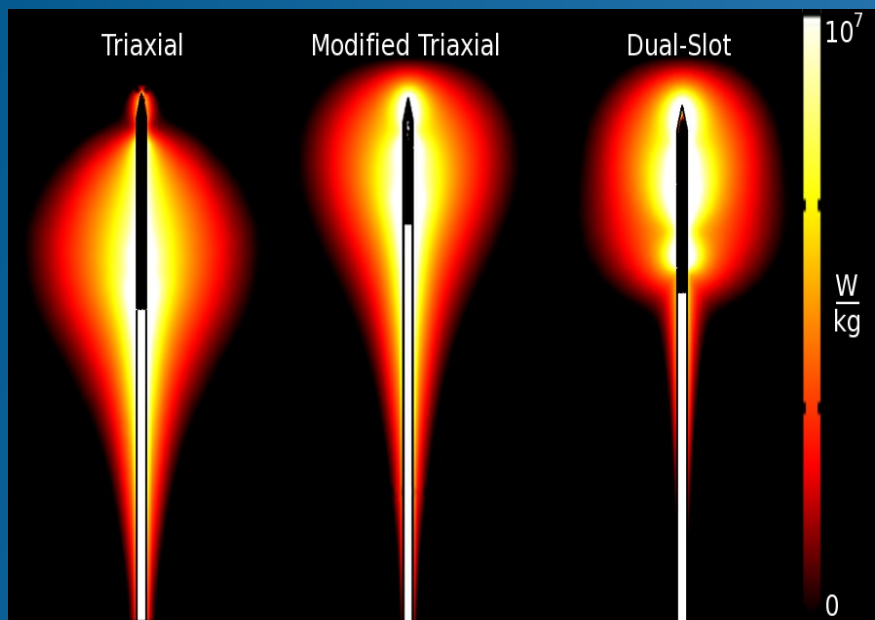
Specify the environment and antenna geometry

Chiang J, Wang P, Brace CL. Computational modelling of microwave tumor ablations. *Int J Hyperthermia*. 2013;29(4):308–317.

Tool Optimization: Organ-specific design

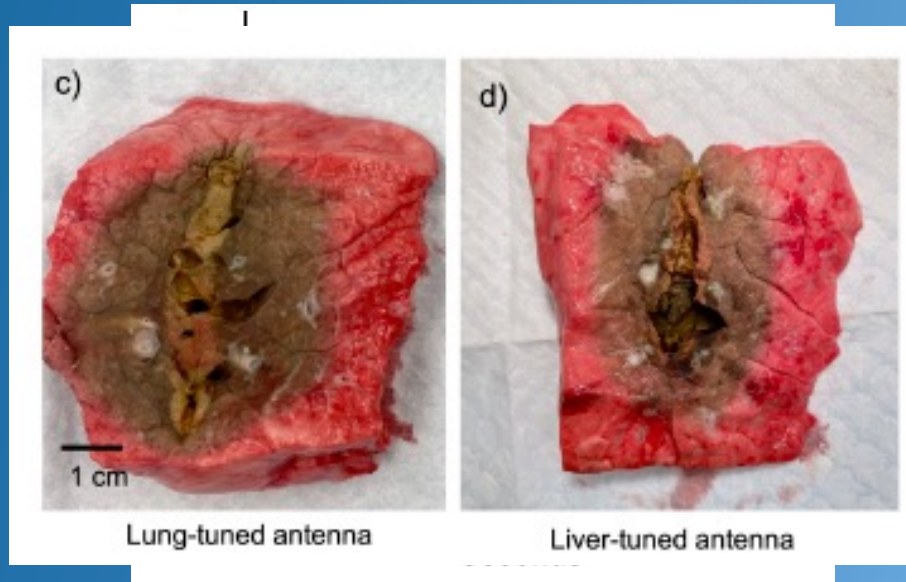
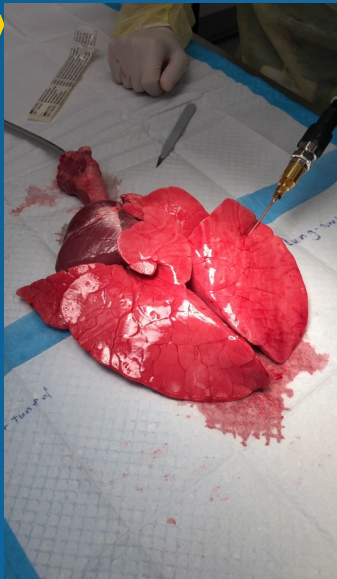


Tool Optimization: Shape-specific design



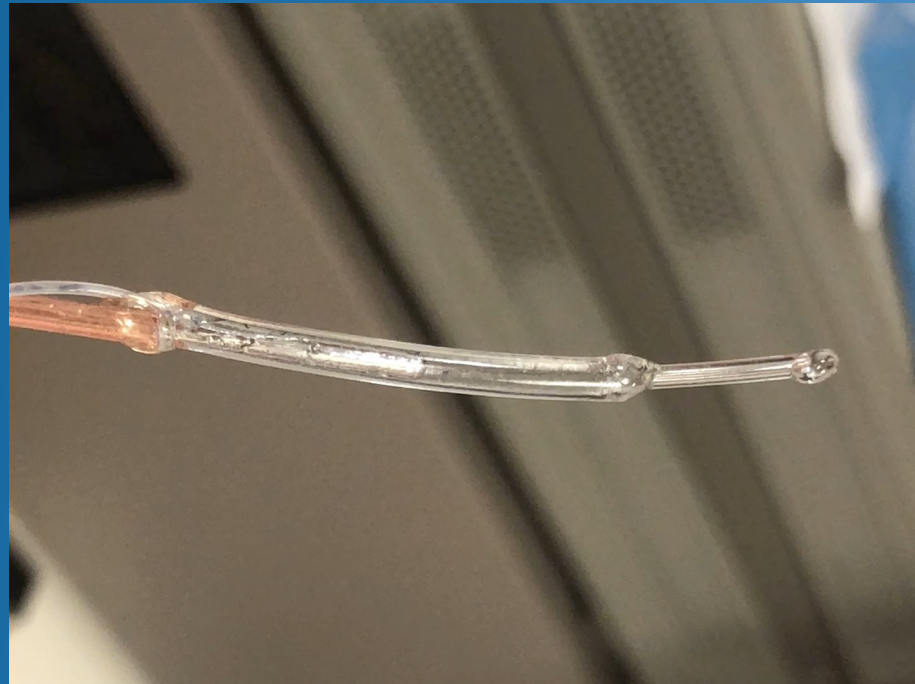
Chiang et al. *Radiology* 268:382-89, 2013.

Comparison between lung-tuned and liver-tuned antennas

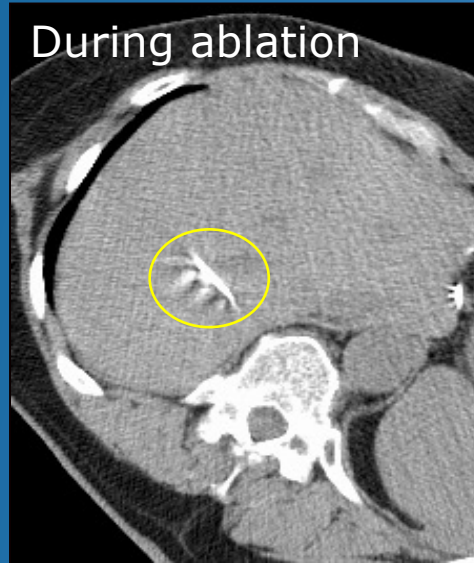
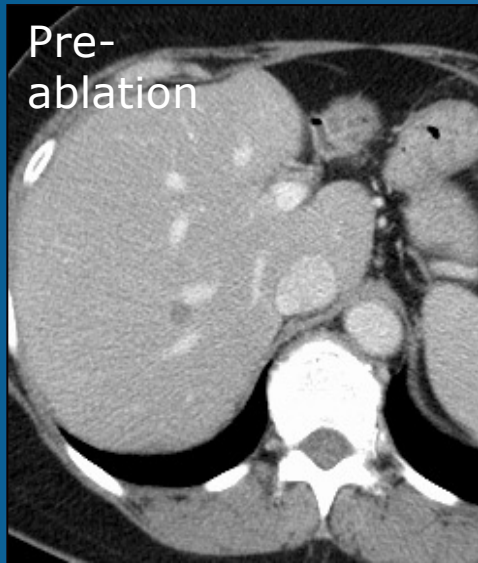


J. Chiang, L. Song, F. Abtin and Y. Rahmat-Samii, "Efficacy of Lung-Tuned Monopole Antenna for Microwave Ablations: Analytical Solution and Validation in a Ventilator-Controlled ex-vivo Porcine Lung Model," in *IEEE Journal of Electromagnetics, RF and Microwaves in Medicine and Biology* (in press)

Tunable Microwave Antennas



Thermal ablations and the heat-sink effect



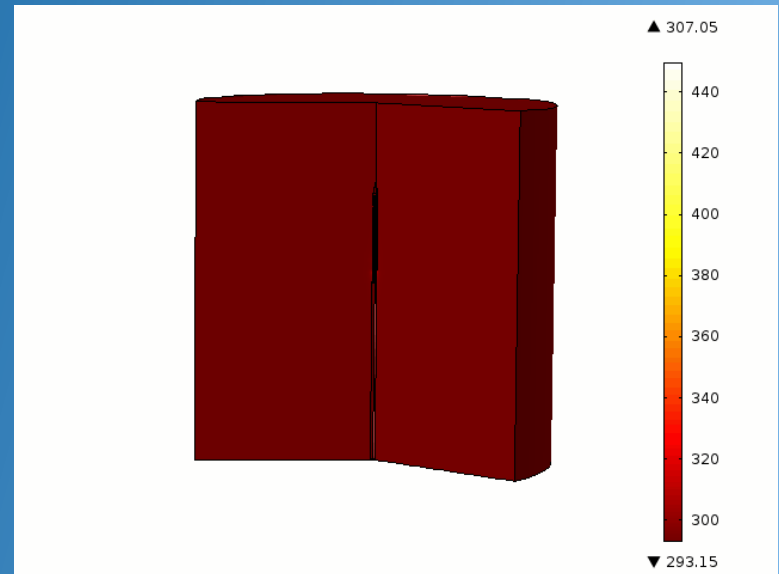
Calculating time-dependent temperature maps



Continuum approach: Use Pennes bioheat equation to create time-dependent ablation isotherms:

$$\nabla \cdot k \nabla T - \rho_b c_b \omega_b (T_{a0} - T) + q_m + Q = \rho c \frac{\partial T}{\partial t}$$

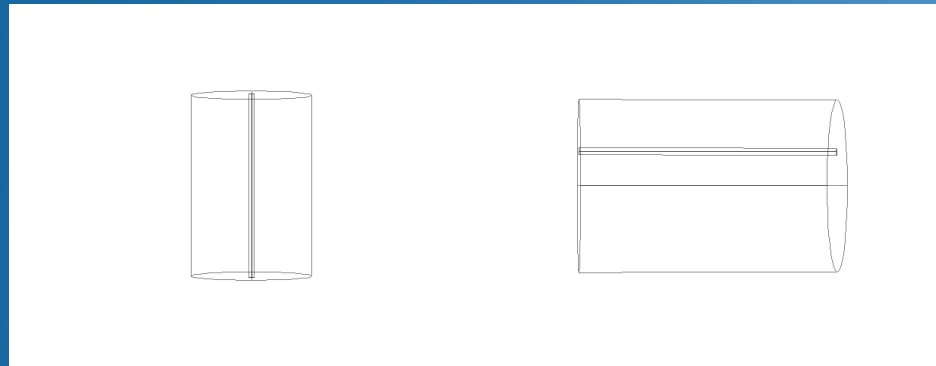
Thermal conduction Blood flow Metabolic heat Heat source



Calculating time-dependent temperature maps



Vascular approach: Model the impact of each vessel individually – mimic the *patient-specific* vascular anatomy for each ablation zone

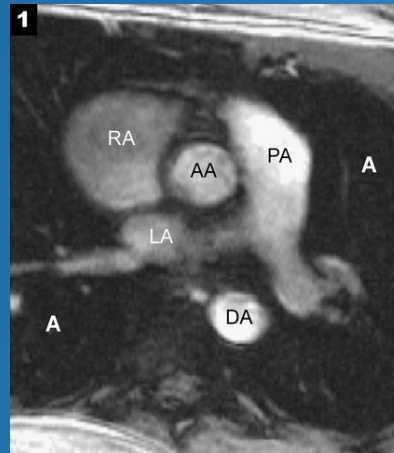


2D Phase Contrast

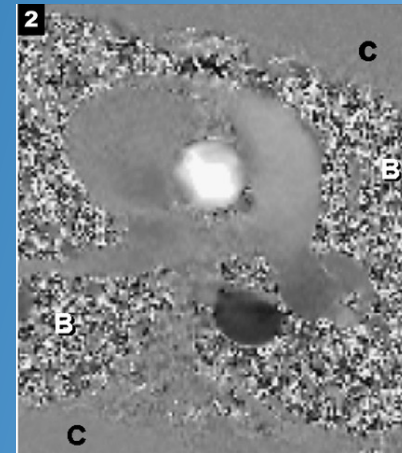
- One directional through-plane (Z) velocity encoding sequence
 - Acquisition of 2 images:
 - ● ● ○ 1 Magnitude image
 - 1 Phase image



Region of Interest: Targeting vessel or anatomy



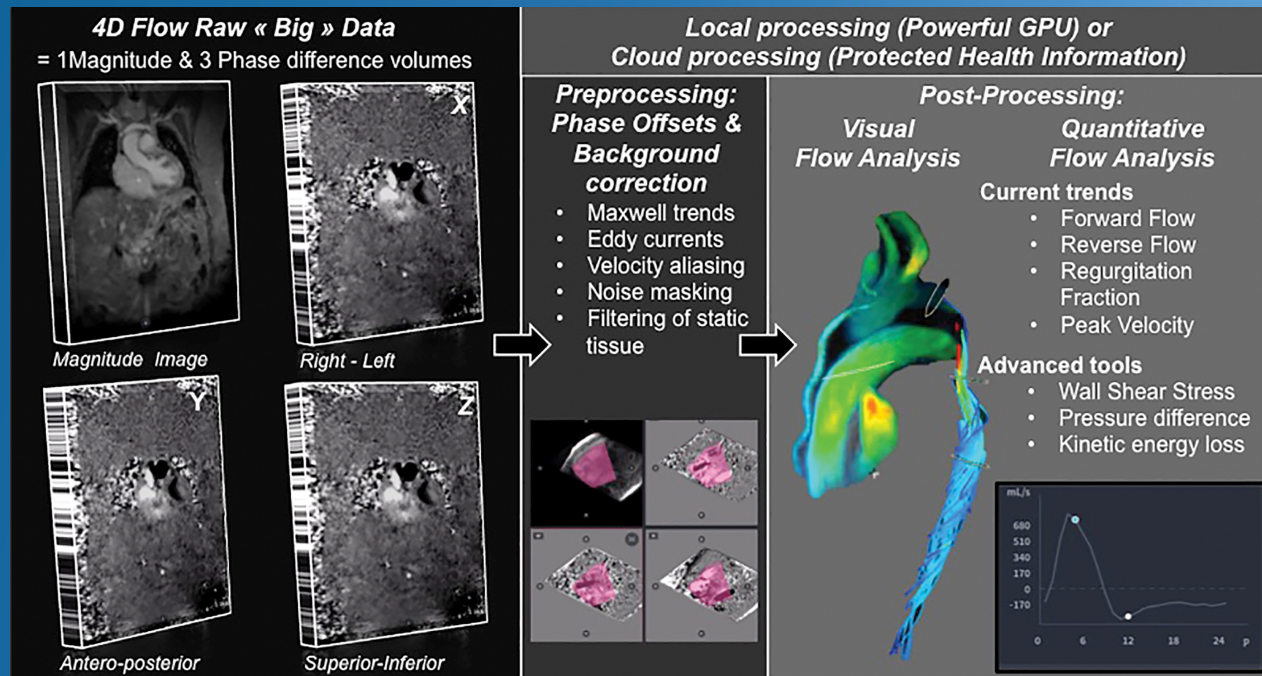
Magnitude image: Signal intensity proportional to **velocity** but no directional information



Phase image: blood flow shows **directional information**

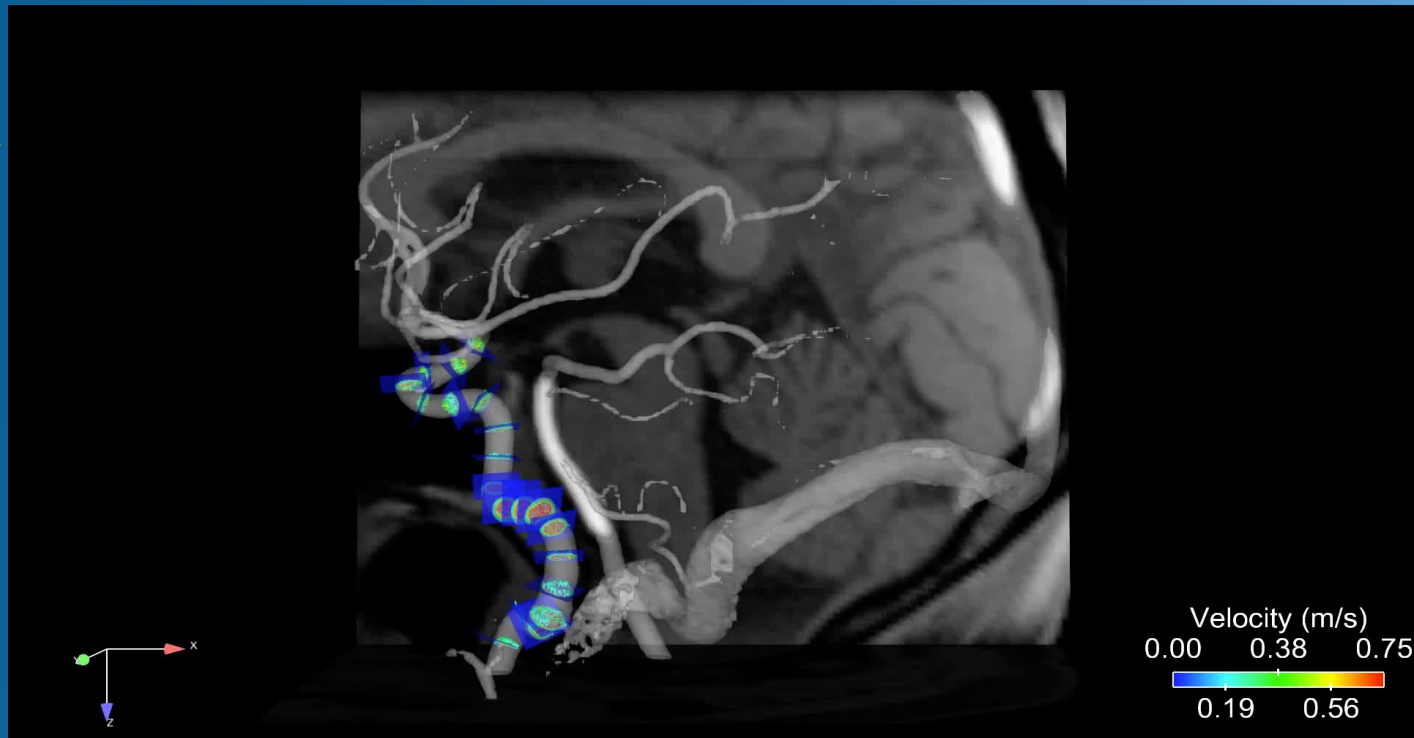
4D flow MRI

- ● ● ●
- One directional through-plane (Z) velocity encoding sequence
 - Acquisition of 4 images: 1 Magnitude image + 3 Phase image



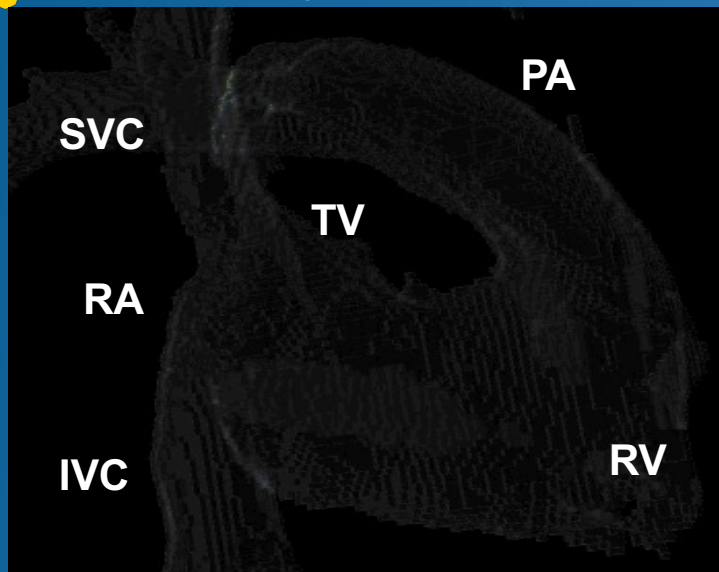
Azarine A, Garçon P, Stansal A, Canepa N, Angelopoulos G, Silvera S, Sidi D, Marteau V, Zins M. Four-dimensional Flow MRI: Principles and Cardiovascular Applications. Radiographics. 2019 May-Jun;39(3):632-648. doi: 10.1148/rg.2019180091. Epub 2019 Mar 22

4D flow MRI: Neuro applications

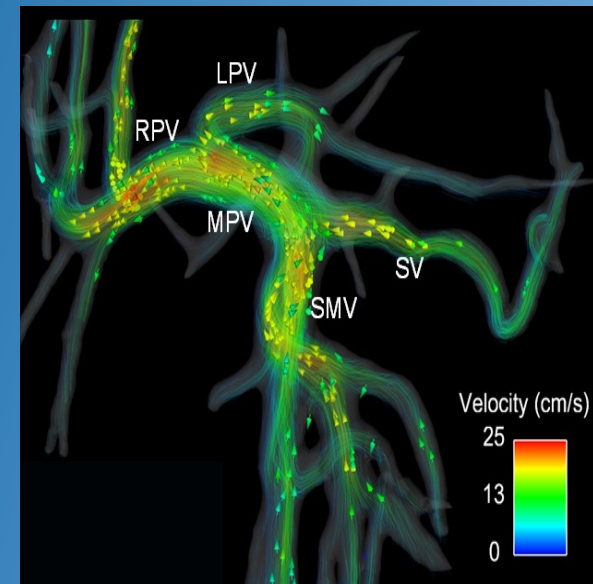


4D flow MRI: Visualizing Flow

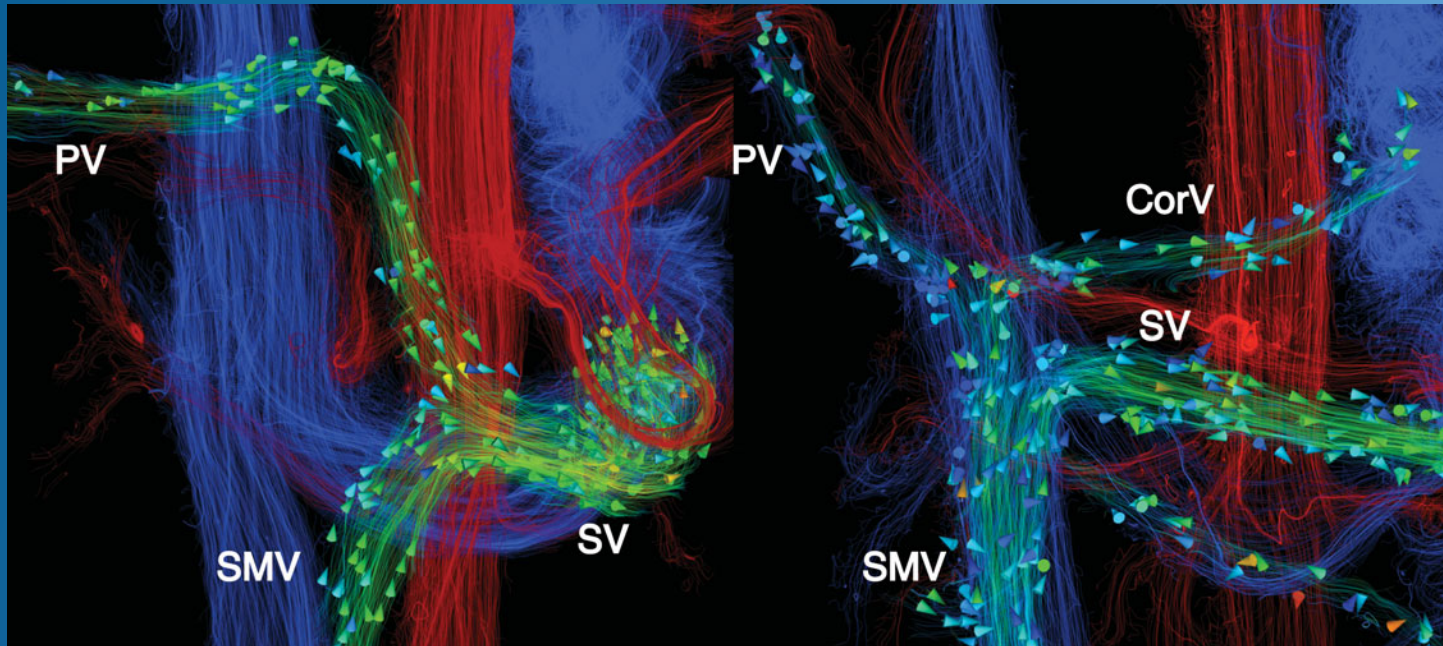
Particle traces in the cardiac system



Streamlines in the Liver



4D flow: Liver Applications



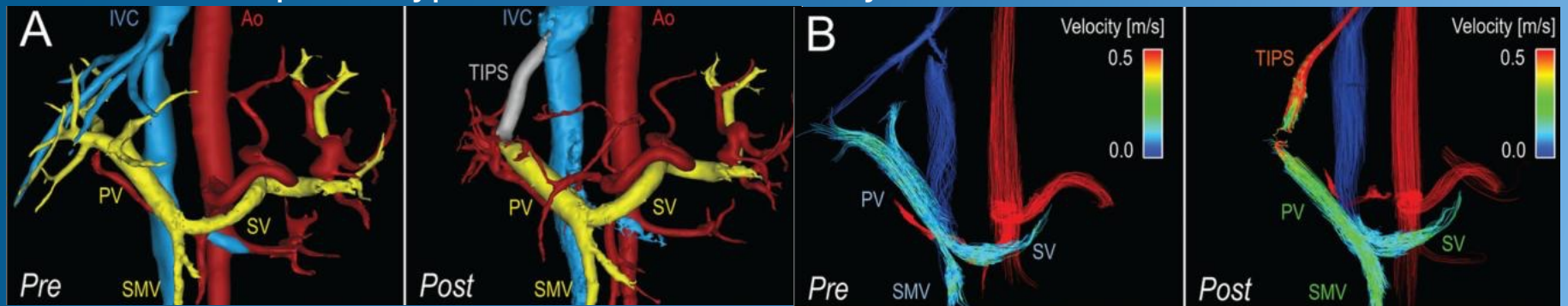
Physiological variation in blood flow through the portal vein due to the increased resistance in two patients with portal hypertension. a: Reversed (hepatofugal) flow is seen in the portal and splenic veins. Conservation of mass analysis showed good agreement (4.57%) between QPV and QSMV \neq QSV. b: Reversed QSV with reduced QPV and normal QSMV.

Hepatic Angiogram showing similar reversal of flow



4D flow: Liver Applications

Four-dimensional–flow MR imaging– based visualization and quantification of hemodynamics in the portal system before and after TIPS placement in a 54-year-old man with portal hypertension and refractory ascites.

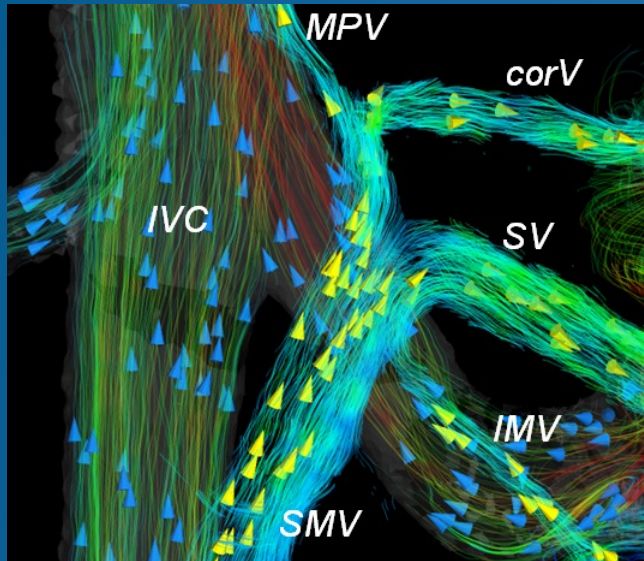


A) Segmentation of 4D-flow angiograms obtained before (pre) and 2 weeks after (post) TIPS placement show arteries (red), veins (blue), portal vasculature (yellow), and TIPS (gray).

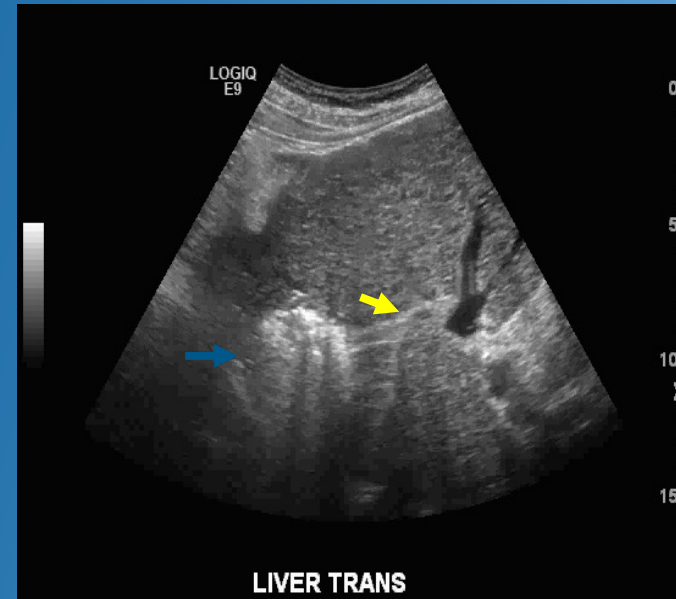
B) Velocity-coded 4D-flow MR images obtained before and 2 weeks after TIPS placement show velocity distribution in the portal circulation. Note the high velocity in the TIPS, with a signal dropout at the proximal end of the TIPS due to disordered flow.

Roldán-Alzate, Alejandro, Christopher J. Francois, Oliver Wieben, and Scott B. Reeder. "Emerging Applications of Abdominal 4D Flow MRI." *AJR. American Journal of Roentgenology* 207, no. 1 (July 2016): 58–66.

4D flow: Ablation-related hemodynamics

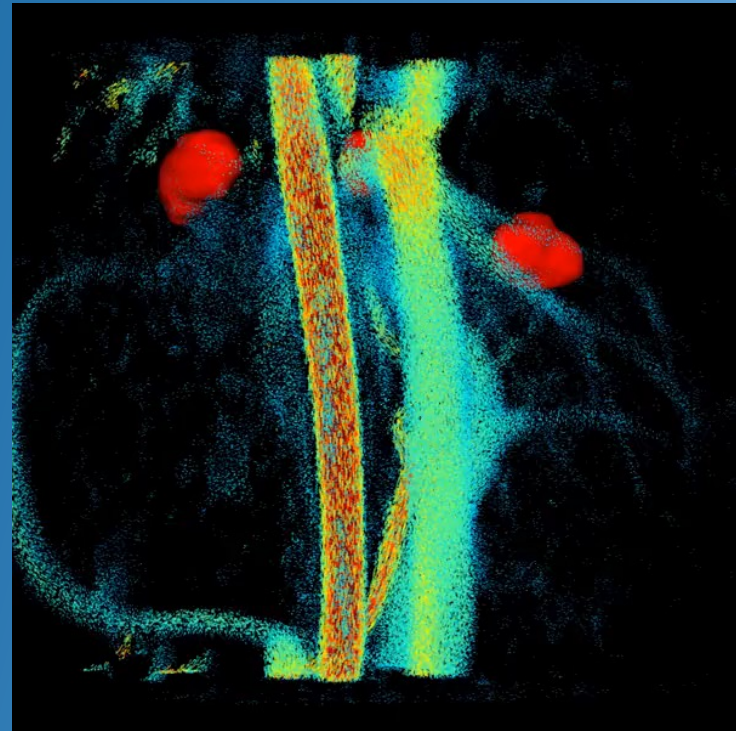


4D Flow images showing flow within the portal veins and IVC.

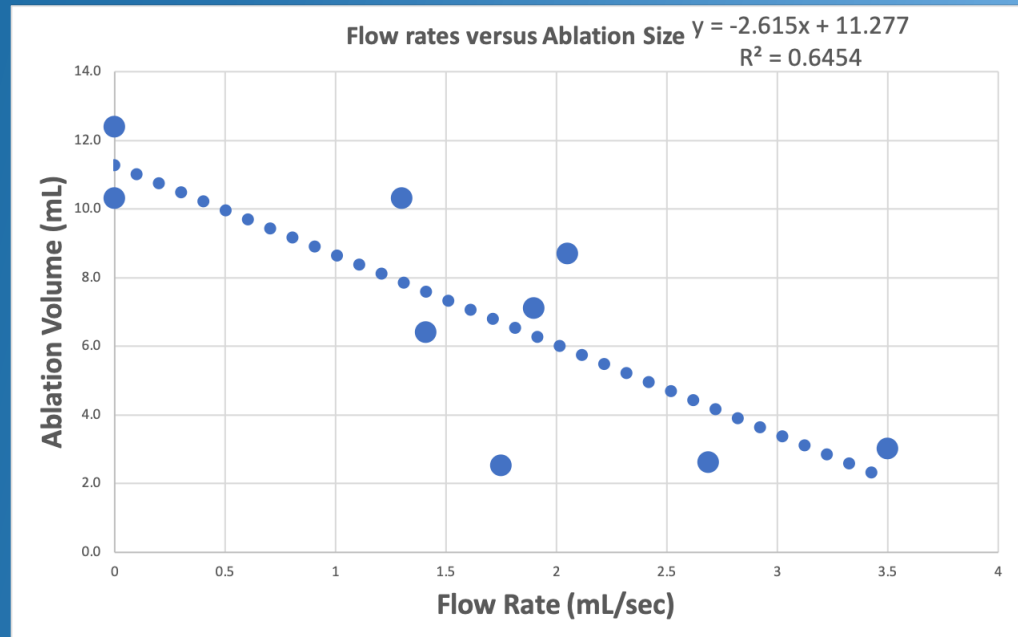
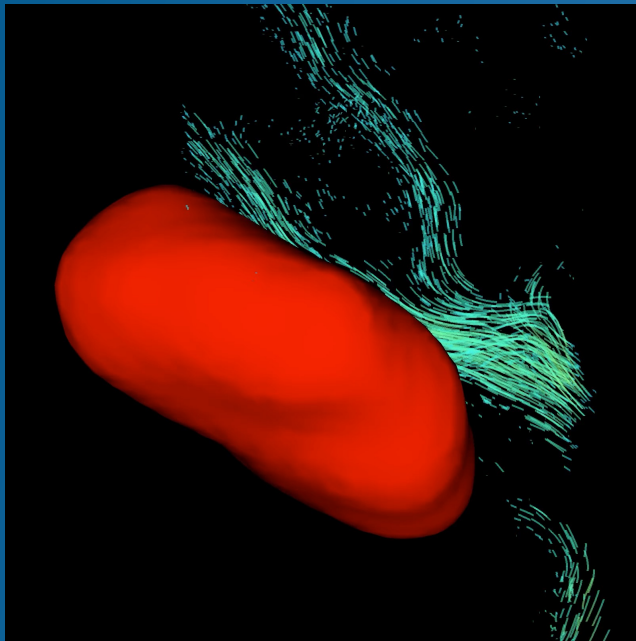


MWA zone (blue arrow) creating water vapor (yellow arrow) that is recondensing while in the hepatic vein.

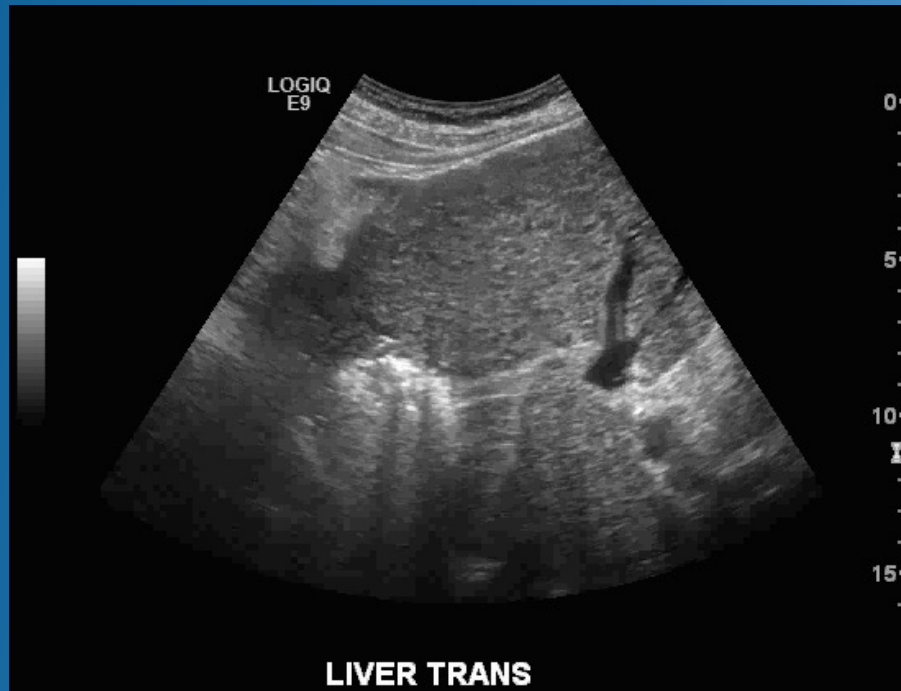
4D flow: Ablation-related hemodynamics



Predicting ablation volume



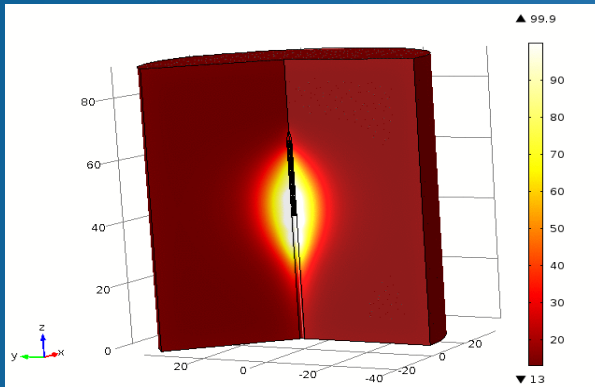
Modeling Heat and Mass Transfer



Modeling MWA: Incorporating water vapor

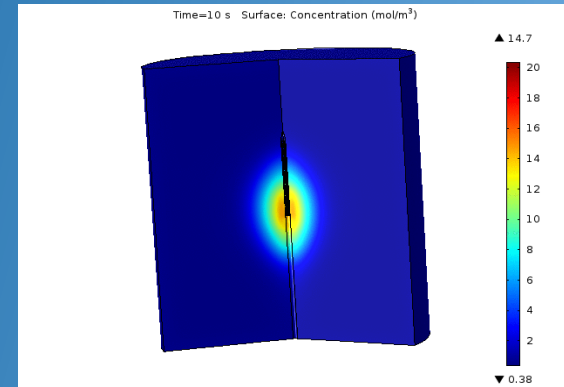
- ● ● Solve heat transfer equation in porous media

$$(\rho c)_{eq} \frac{\partial T}{\partial t} + \rho_L c_{\rho L} \mathbf{u} \cdot \nabla T = \nabla \cdot (k_{eq} \nabla T) + Q$$



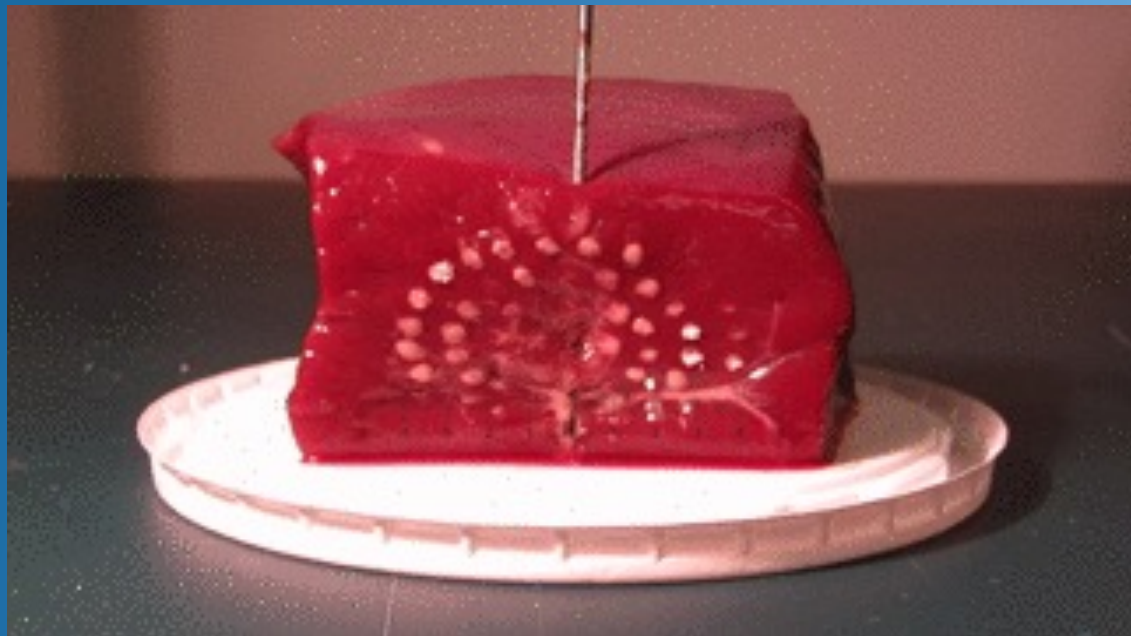
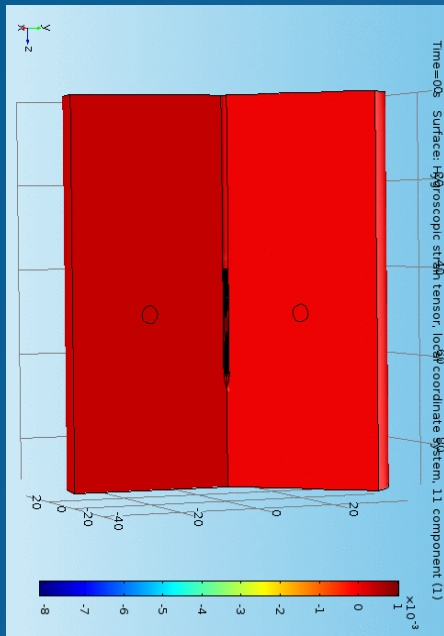
- Solve for liquid water and water vapor diffusion through liver tissue

$$\frac{\partial c}{\partial t} + \mathbf{u} \cdot \nabla c = \nabla \cdot (D \nabla c) + R$$

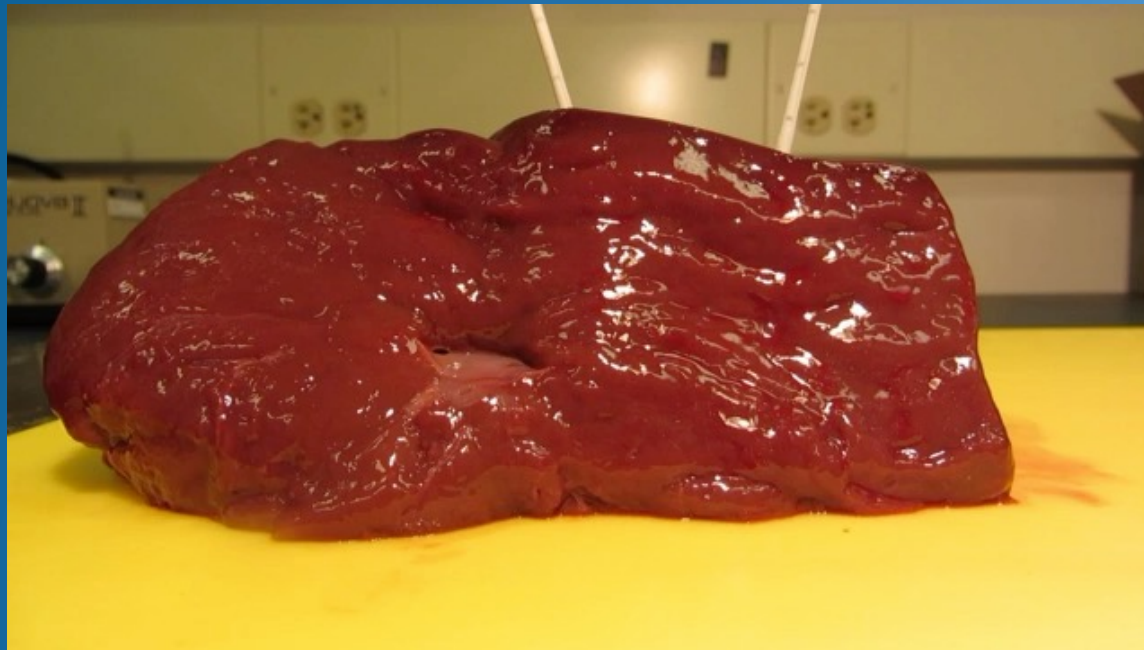


Chiang, Jason, Sohan Birla, Mariajose Bedoya, David Jones, Jeyam Subbiah, and Christopher L. Brace. "Modeling and Validation of Microwave Ablations with Internal Vaporization." *IEEE Transactions on Bio-Medical Engineering* 62, no. 2 (February 2015): 657–63.

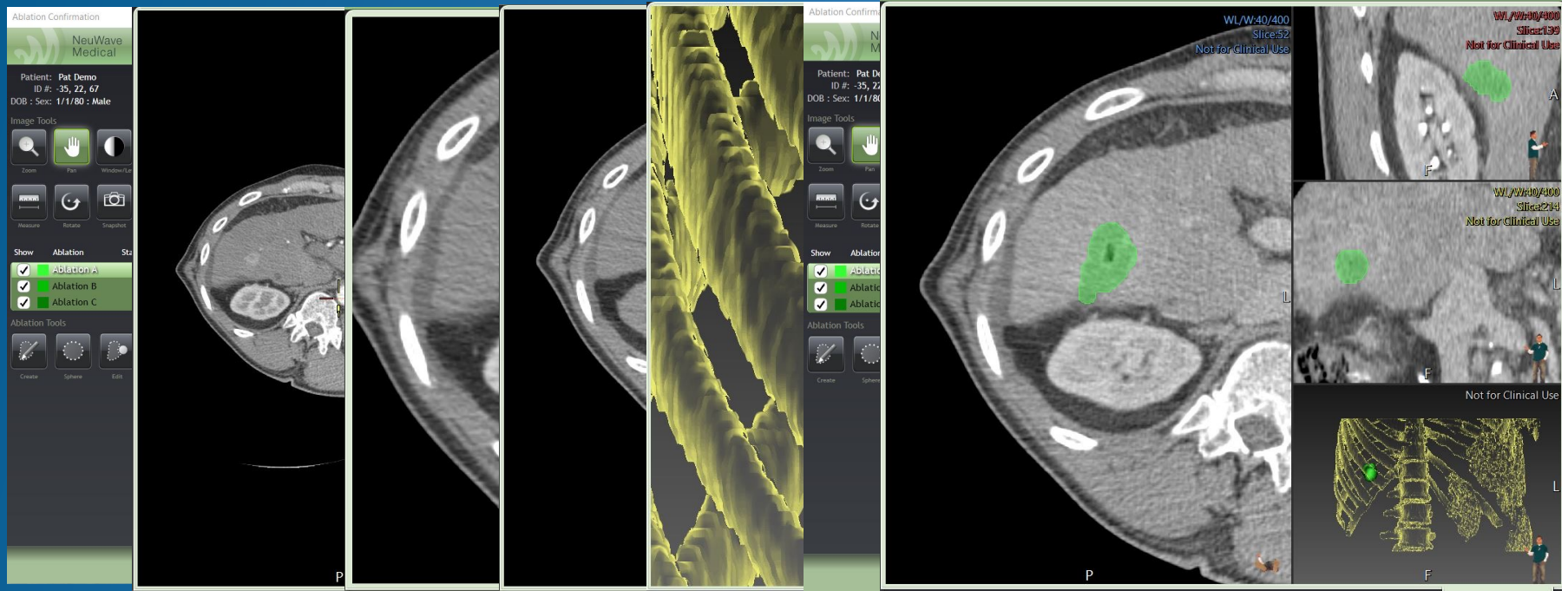
Water vapor diffusion = Contraction



Contraction in Clinical Practice

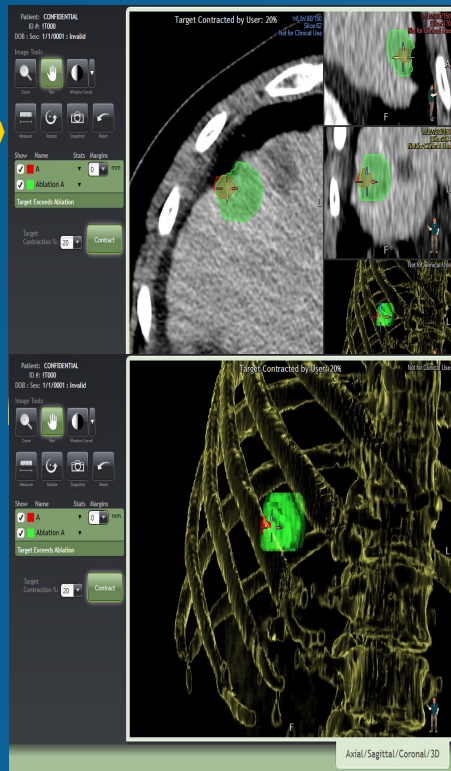


Current state of microwave planning and modeling



Integrating contraction into MWA planning

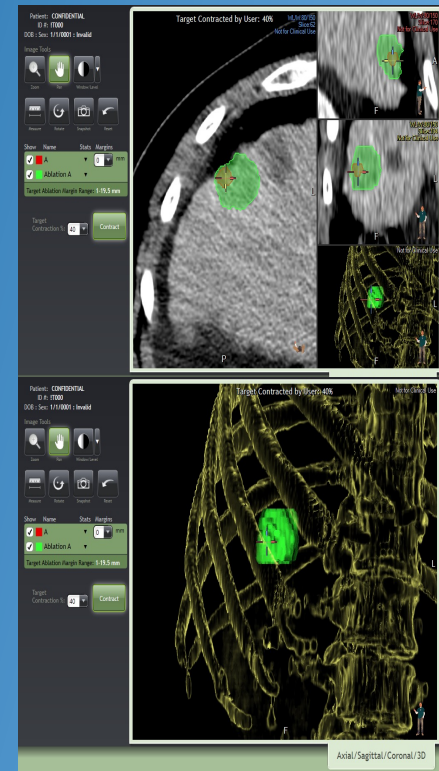
20%



30%



40%



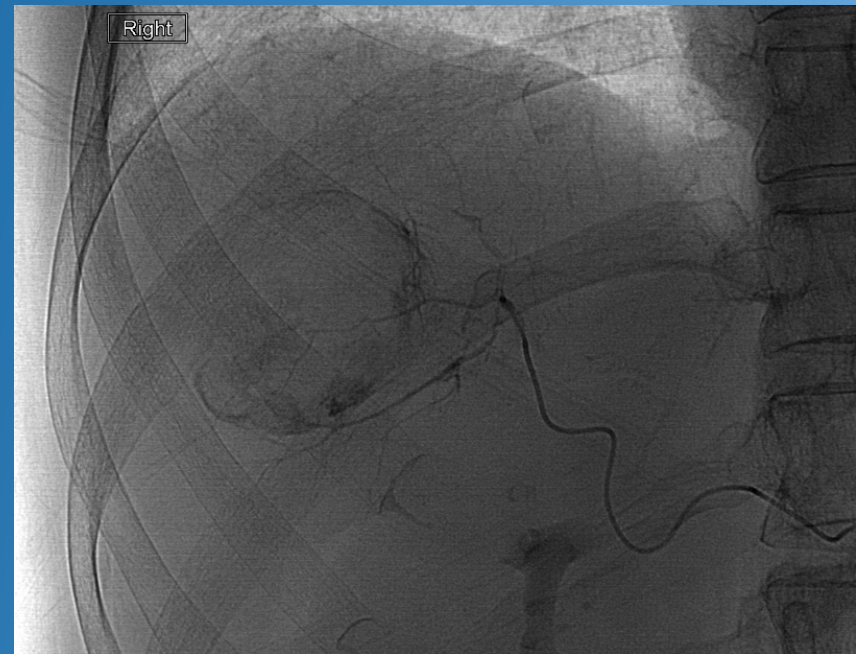
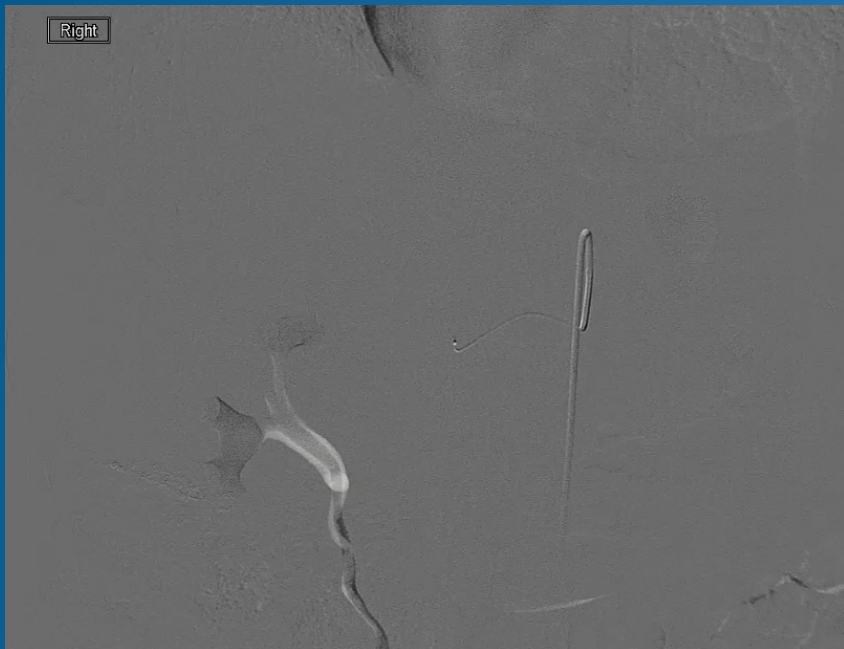
Back to original case: Diagnostic evaluation

8/27

10/15



Transarterial chemoembolization + ablation



Post-embolization ablation



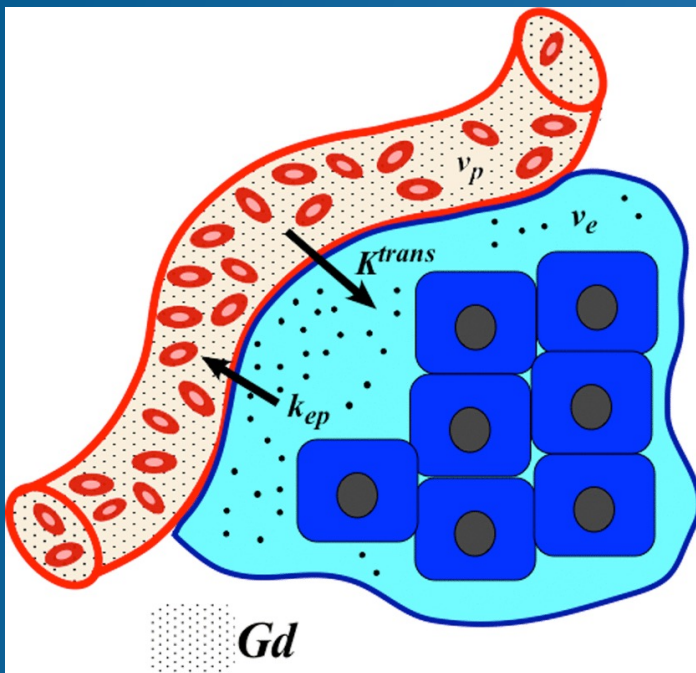
Post-ablation CT scan



Perfusion MRI



Modeling Perfusion with Tofts model



$$C_t(t) = v_p C_p(t) + K^{trans} \int_0^t C_p(\tau) e^{-(K^{trans}/v_e)(t-\tau)} d\tau$$

- $C_t(\tau)$ is the total tissue contrast agent concentration
- $C_p(t)$ is the time-varying blood plasma concentration after a bolus of gadolinium is administered
- K_{trans} (min^{-1}) is the forward rate constant
- k_{ep} (min^{-1}) is the backward rate constant.

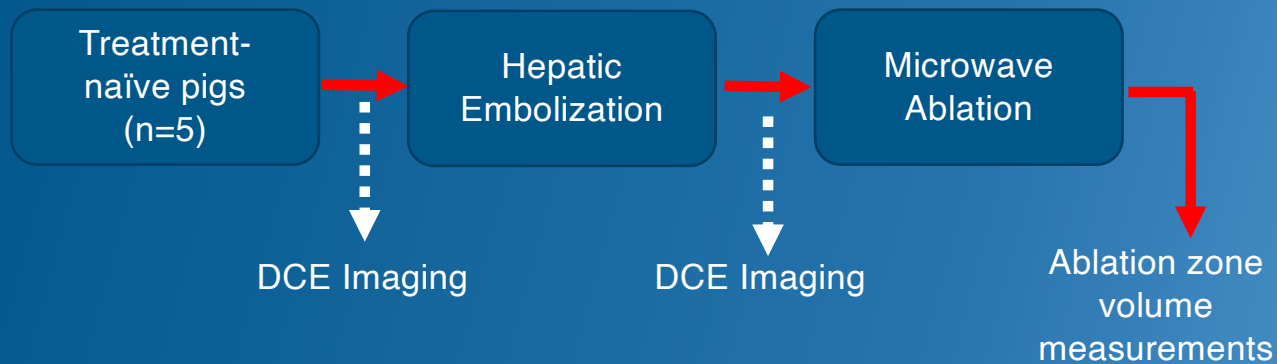
Calculating free parameters K_{trans} and k_{ep} required an assumption of the arterial plasma concentration $C_p(t)$, for which a population-derived arterial input function

Study Question

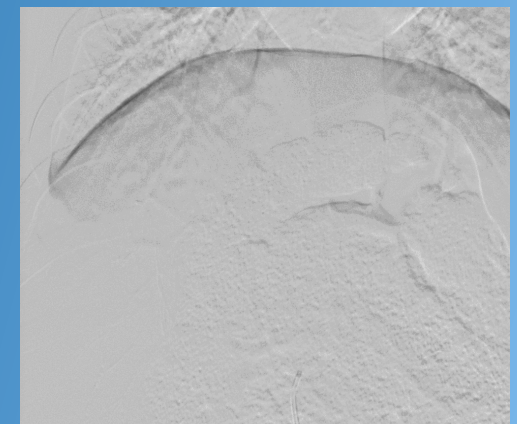


Can **pre-ablation perfusion MRI** predict the **microwave ablation zone sizes** near liver vessels in an in-vivo liver model?

In Vivo Study Design



Study goal:
Correlation of post-embolization perfusion with ablation volume in combination therapy

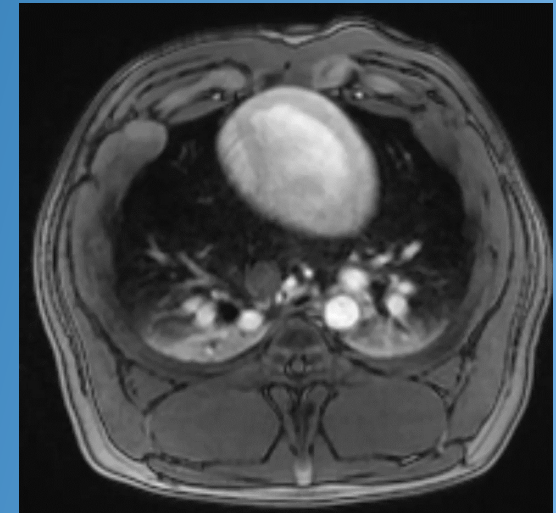
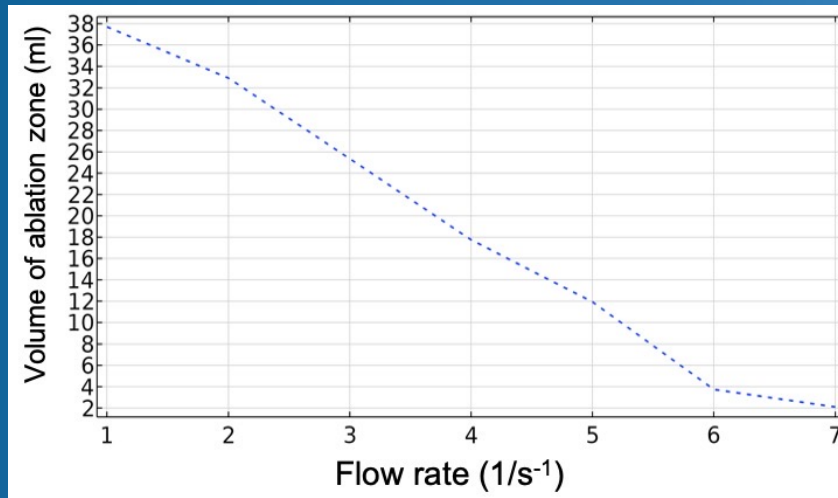


Modeling the effects of perfusion

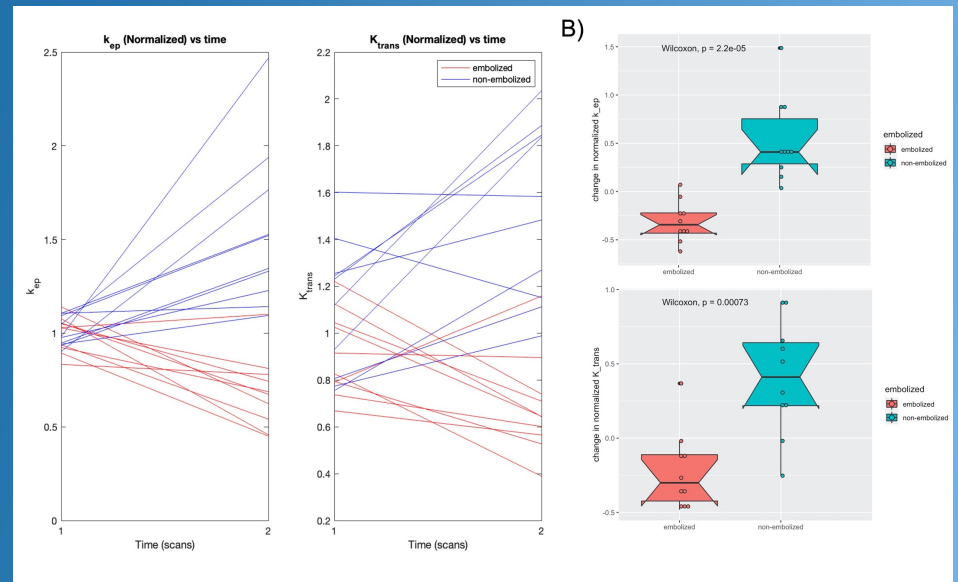
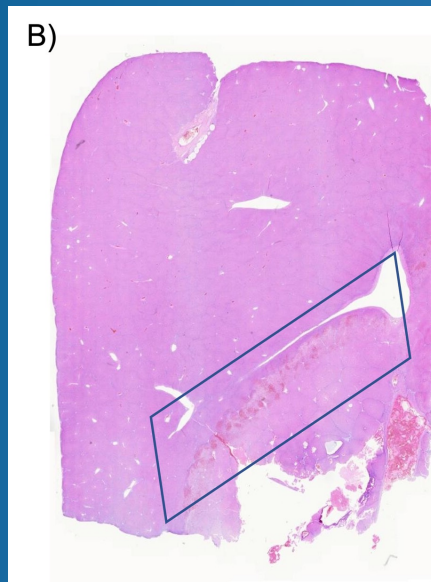
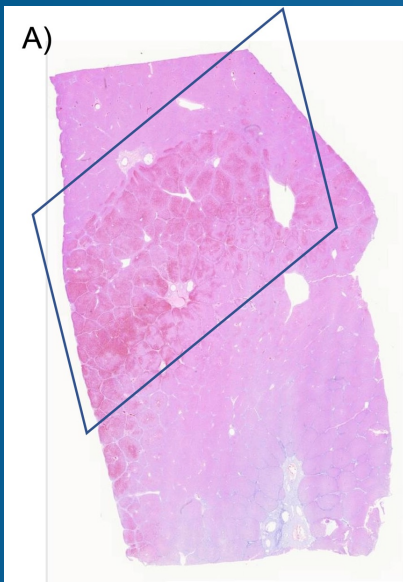
$$\bullet \bullet \bullet \nabla \cdot k \nabla T - \rho_b c_b \omega_b (T_{a0} - T) + q_m + Q = \rho c \frac{\partial T}{\partial t}$$

Heat source

Thermal conduction
Blood flow
Metabolic heat

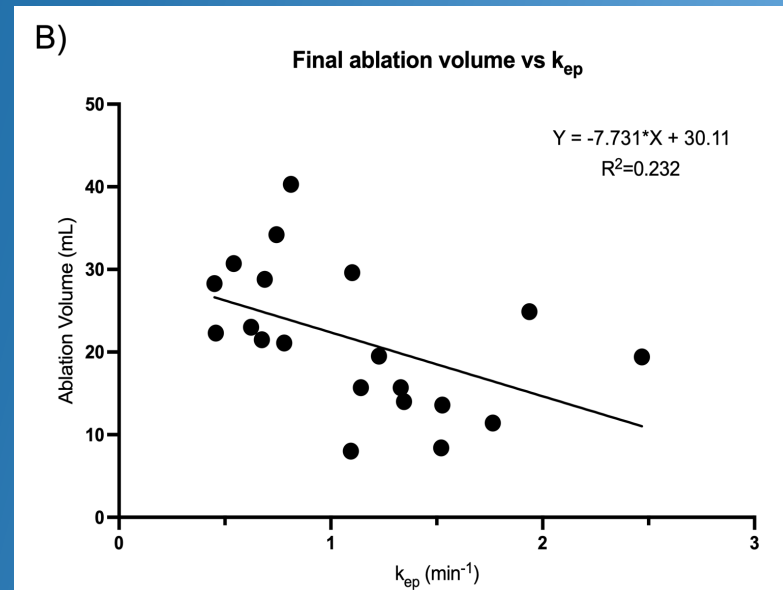
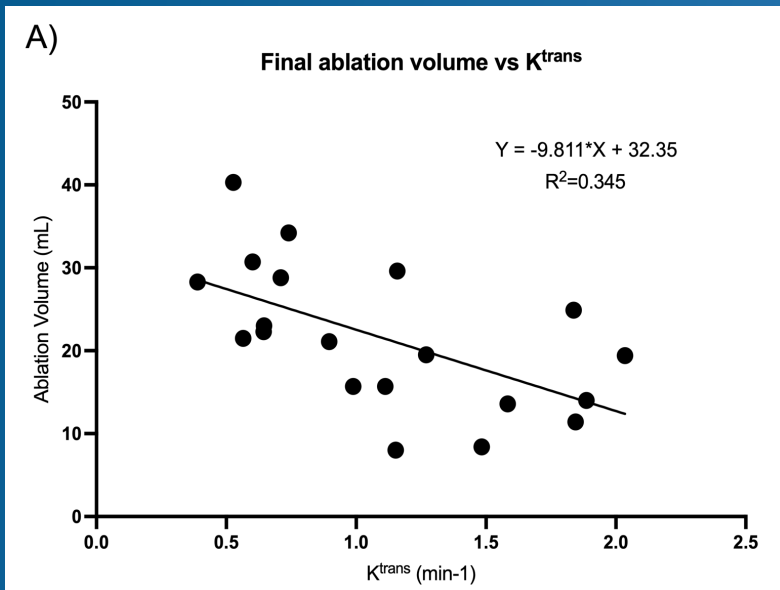


Histopathology and modeling



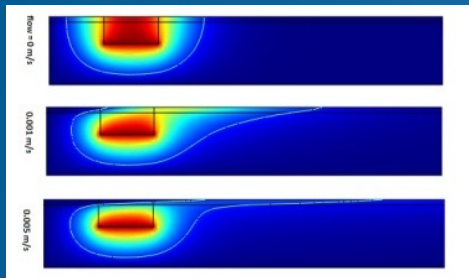
Chiang J, Sparks H, Rink JS, Meloni MF, Hao F, Sung KH, Lee EW. Dynamic Contrast-Enhanced MR Imaging Evaluation of Perfusional Changes and Ablation Zone Size after Combination Embolization and Ablation Therapy. J Vasc Interv Radiol. 2023 Feb;34(2):253-260. doi: 10.1016/j.jvir.2022.10.041.

Correlating DCE-MRI parameters with ablation volume



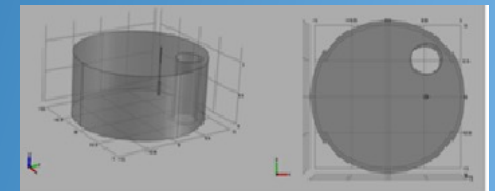
Chiang J, Sparks H, Rink JS, Meloni MF, Hao F, Sung KH, Lee EW. Dynamic Contrast-Enhanced MR Imaging Evaluation of Perfusional Changes and Ablation Zone Size after Combination Embolization and Ablation Therapy. J Vasc Interv Radiol. 2023 Feb;34(2):253-260. doi: 10.1016/j.jvir.2022.10.041.

Validation of numerical models



Increasingly complicated numerical models

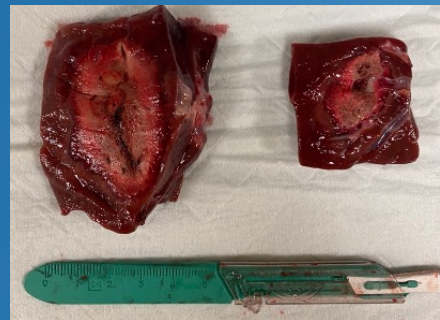
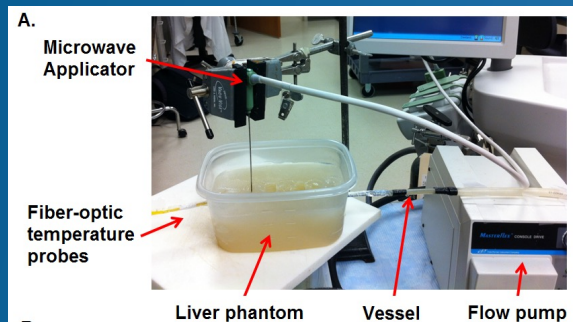
Model Validation



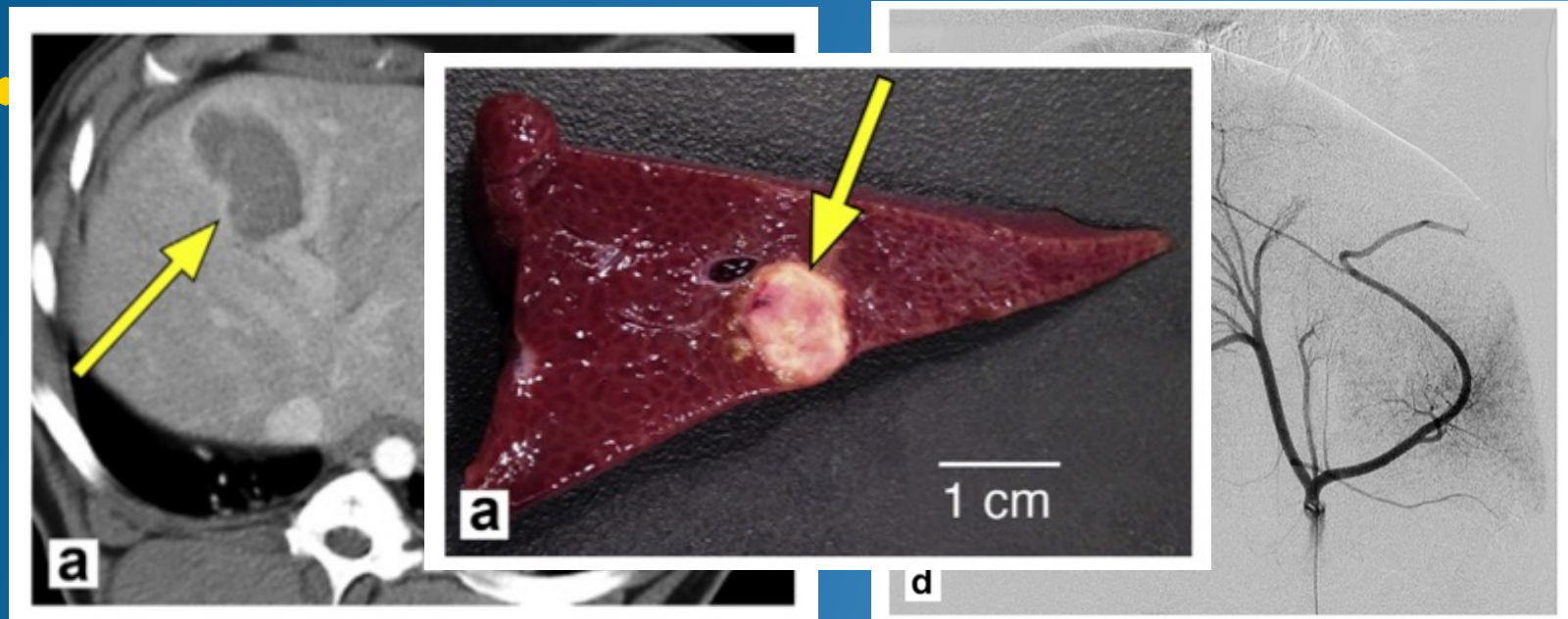
Phantom models

Ex vivo tissue models

In vivo tissue models

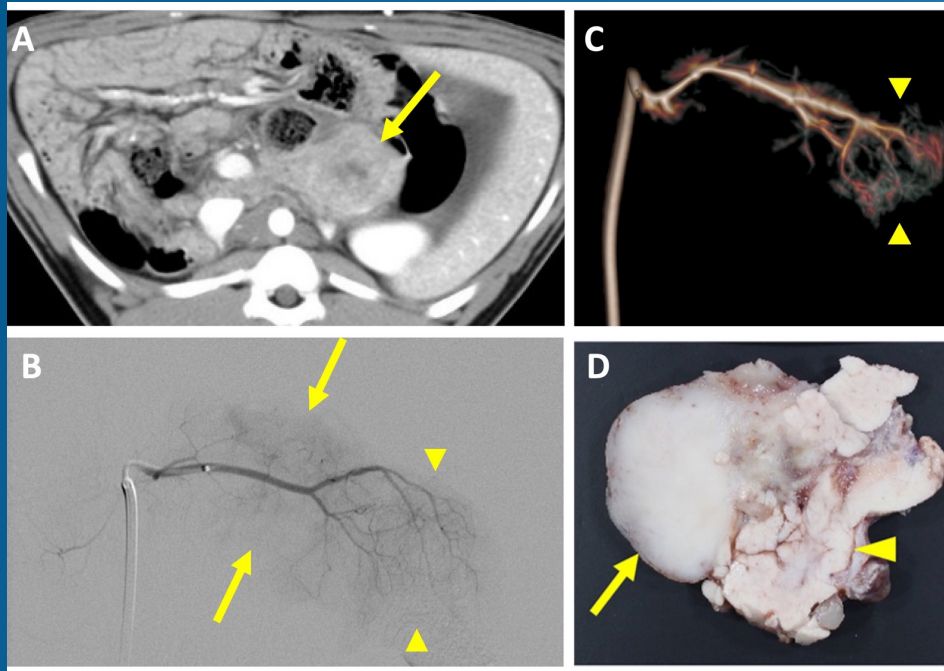


Oncopig tumor model



Nurili F, Monette S, Michel AO, Bendet A, Basturk O, Askan G, Cheleuitte-Nieves C, et al. Transarterial Embolization of Liver Cancer in a Transgenic Pig Model. *J Vasc Interv Radiol.* 2021 Apr;32(4):510-517.e3.

Oncopig validation of immunoadjuvant therapy



- Oncopig contains **P53 and Kras** mutations, common mutations seen in human pancreatic ductal adenocarcinoma.
- “**Immune cold**” tumor – lowest response rates to current immunotherapies
- The immune response can be potentiated with the immunostimulant CpG oligodeoxynucleotides (ODN)
 - **TLR9 agonist** that can induce powerful dendritic cell antigen presentation and proinflammatory cytokine production

Summary: MR guided interventions

- Modeling of microwave ablations can **more accurately characterize the impact of energy delivery strategies** in a complex biological environment.
 - **Patient-specific parameters** (vascular anatomy, tissue properties, water vapor movement, contraction)
 - Give physicians a **tool to predict when more aggressive needle placement or power settings** are warranted.
 - Repeat in silico instead of in patient.
- **Fusion imaging** can facilitate the adoption of numerical modeling into current ablation workflow
- **Validation is critical to any model** – large animal model studies required to truly move the needle forward

Acknowledgements



- NIH
 - F30 CA165548
 - UL1TR001881
- UCLA Department of Radiology
- UCLA Clinical and Translational Science Institute (CTSI)
- University of Wisconsin Department of Radiology
- Radiological Society of North America





Thank You